

## Research Article

## Effect of Pre-Heat Treatment and Processing Regime on the Behavior of Aluminum Alloy 2024 During Equal Channel Angular Pressing

E. Ramesh, M.H. Farshidi\* and A. Rezaee-Bazzaz

Department of Materials Science and Engineering, Ferdowsi University of Mashhad, Azadi Square, Mashhad, Iran

## ARTICLE INFO

*Article history:*

Received 29 December 2024  
 Reviewed 11 January 2025  
 Revised 1 February 2025  
 Accepted 5 February 2025

*Keywords:*

AA2024  
 Severe plastic deformation  
 Heat treatment  
 Processing regime

*Please cite this article as:*

Ramesh E., Farshidi, M. H., & Rezaee-Bazzaz, A. (2024). Effect of pre-heat treatment and processing regime on the behavior of aluminum alloy 2024 during equal channel angular pressing. *Iranian Journal of Materials Forming*, 11(4), 27-33.  
<https://doi.org/10.22099/IJMF.2025.52025.1315>

## ABSTRACT

Aluminum alloy 2024 is widely used in various industries, making its strengthening a critical area of research. Severe plastic deformation (SPD) has emerged as a promising method for enhancing the mechanical properties of AA2024; however, few studies have examined the influence of processing parameters on its microstructure evolution and mechanical performance during SPD. In this study, the effects of pre-processing heat treatment and deformation regime on AA2024 during equal channel angular pressing (ECAP) were investigated. The alloy was subjected to two different heat treatments prior to ECAP and processed at two distinct temperatures. Optical microscope (OM) and scanning electron microscopy (SEM) were used to monitor microstructure changes, while Vickers hardness testing evaluated the hardness variation following processing. The results reveal that multiple ECAP passes can only be applied successfully after overaging, as the workability of the alloy is compromised following solution treatment. Furthermore, increasing the processing temperature from 25 °C to 150 °C has a limited effect on the alloy's behavior.

© Shiraz University, Shiraz, Iran, 2024

## 1. Introduction

Aluminum 2xxx alloys (AA2xxx) are widely used in different industries—such as aircraft and high-speed train manufacturing—due to their unique mechanical properties. These alloys typically contain copper (Cu) and magnesium (Mg) as the primary alloying elements. The presence of these elements promotes the formation

of  $\text{CuAl}_2$  and  $\text{CuMgAl}_2$  precipitates through the following sequence of steps [1-3]:

$$\text{Supersaturated Solid Solution (SSS)} \rightarrow \text{GP Zones} \rightarrow \theta'' \rightarrow \theta' \rightarrow \theta(\text{CuAl}_2)$$

$$\text{Supersaturated Solid Solution (SSS)} \rightarrow \text{GP Zones} \rightarrow S' \rightarrow S(\text{CuMgAl}_2)$$

These precipitates increase the strength of the alloys,

\* Corresponding author  
 E-mail address: [farshidi@um.ac.ir](mailto:farshidi@um.ac.ir) (M.H. Farshidi)  
<https://doi.org/10.22099/IJMF.2025.52025.1315>

serving as a key strengthening mechanism for AA2xxx alloys. In addition to Cu and Mg, other alloying elements like manganese (Mn) and zirconium (Zr) are sometimes added to control grain growth. The lower grain size increases different mechanical properties of the alloys, including strength, fracture toughness, and fatigue resistance. For instance, AA2024, the most commonly used alloy in this series, typically contains about 4.5 wt.% Cu, 1.5 wt.% Mg, and 0.6 wt.% Mn. This alloy is extensively employed in manufacturing aircraft frames, wings, and fuselage shells [1-6]. Given the importance of AA2024, numerous studies have sought to enhance its mechanical properties through different methods such as precipitation heat treatment, thermomechanical processing, and the incorporation of particles or fibers [5-8]. However, relatively few investigations have considered a combination of these methods to further strengthen the alloy.

In recent decades, the concept of thermomechanical processing has been expanded by introducing severe plastic deformation (SPD). Today, the SPD is an outstanding method to increase the strength and other mechanical properties such as fatigue resistance. SPD is defined as the imposition of a considerable plastic strain (typically exceeding a strain value of 2) through cold or warm deformation regimes. The modern usage of SPD began in the 1970s when Segal et al. introduced a process called equal channel angular pressing (ECAP) [9-13]. SPD typically yields significant strengthening by refining the grain size and increasing the density of crystal defects such as dislocations. As a result, numerous studies have considered the SPD as a strengthening method for aluminum alloys [12-15]. Among wrought aluminum alloys, the 6xxx series (AA6xxx) has received considerable attention due to its precipitation hardening capability, which may produce a synergetic effect when combined with the strengthening provided by SPD [13, 16]. However, this approach has rarely been applied to AA2xxx alloys.

This work aims to investigate the possibility of combining the strengthening effects of severe plastic deformation (SPD) with those of precipitation heat treatment for AA2024. To this end, the effects of pre-

SPD heat treatments and different processing regimes on the behavior of AA2024 during equal channel angular pressing are investigated. Two distinct heat treatments are applied prior to ECAP, and the process is conducted at two different temperatures. The microstructure of the specimens is observed using optical microscopes (OM) and scanning electron microscopes (SEM), while changes in hardness are evaluated using the Vickers method.

## 2. Materials and Methods

A circular rod of AA2024 with a diameter of 10 mm was obtained for this study. The chemical composition was determined using optical emission spectrometry, and the results are presented in Table 1. The rod was subsequently cut into 75 mm-long specimens and subjected to a solution treatment at 530 °C for 2 hours. Thereafter, the ECAP processing was performed according to one of the following procedures:

- 1- SS: Specimens were processed immediately by ECAP after the solution treatment.
- 2- OVG: Specimens were overaged at 300 °C for 2 hours prior to ECAP processing.

ECAP processing was carried out for up to four passes under two different regimes: cold deformation at 25 °C and warm deformation at 150 °C. Each specimen was labeled with a code indicating the number of ECAP passes, the processing procedure, and the applied ECAP temperature. For example, 1SS25 designates the specimen that underwent one pass of ECAP at 25 °C following the SS procedure. Fig. 1 illustrates the ECAP die set used in this study. The die features a channel with a diameter of 10.1 mm, a corner angle of 90°, and a corner radius of 2.5 mm. Each pass through the die imposes an equivalent plastic strain of approximately 0.9. Additional technical details regarding the ECAP die and processing procedure are presented in [17, 18]. Following ECAP processing, the specimens were subjected to Vickers hardness testing using a 20 N load with each measurement at least 5 times per specimen.

For optical microscopy (OM) analysis, specimens were cut, mechanically polished, and etched using Keller's etchant. The microstructures of the specimens

were then observed using a BX-60M optical microscope. In addition, scanning electron microscopy (SEM) observations were carried out with a TESCAN MIRA3-XMU instrument. During SEM analysis, electron channeling contrast imaging (ECCI) was used to assess grain size, while energy-dispersive X-ray spectroscopy (EDXS) was used to evaluate the chemical composition of the precipitates. Microstructural quantification was performed using MIP5 image analysis software.

**Table 1.** The chemical composition of the received alloy

Element	Al	Si	Fe	Cu	Mn	Mg	Zn
Concentration (wt.%)	Rem.	0.11	0.42	3.81	0.51	1.29	0.24



**Fig. 1.** The ECAP die set used in the present work.

### 3. Results and Discussion

Fig. 2 shows specimens processed using the SS procedure. After two passes of Capsomere, localized macroscopic cracks are evident, and after four passes, an overall fracture is observed. In contrast, specimens processed with the OVG procedure for four passes of ECAP exhibit no macroscopic cracks. Fig. 3 compares the optical microscopy (OM) microstructures of the alloy before and after ECAP processing using the SS procedure. As shown in Fig. 3(a), the alloy initially exhibits relatively coarse grains. In Fig. 3(b), the microstructure of the 1SS25 specimen is characterized by elongated grains and the presence of micro-shear bands. After the second pass, macro-shear bands appeared in the microstructures, as illustrated in Figs. 3(c) and 3(d). These macro-shear bands likely explain the macroscopic cracks observed in the SS processed specimens shown in Fig. 2. This behavior is attributed to dynamic strain aging (DSA) in AA2xxx alloys. In a

supersaturated AA2xxx, GP zones and fine precipitates form rapidly and are subsequently sheared by dislocations, leading to localized negative strain-hardening. Moreover, the alloy's flow stress shows only a weak dependence on the strain rate [19-21]. Together, these phenomena promote strain localization, which leads to the formation of macroscopic shear bands and, ultimately, cracking [22, 23]. Based on these results, the applicability of the SS procedure for ECAP processing of AA2024 appears to be limited. Fig. 4 displays the microstructures of specimens processed using the ECAP-OVG procedure as observed by SEM-ECCI. A comparison between Fig. 3(a) and Fig. 4 clearly demonstrates that a considerable grain refinement is obtained using ECAP-OVG. Table 2 lists the average grain sizes for the specimens presented in Fig. 4. The data indicate that the average grain size is reduced to approximately 3  $\mu\text{m}$  after two passes of ECAP-OVG and further decreases to about 1  $\mu\text{m}$  after four passes. These findings are consistent with previous studies on this alloy [24-28] and can be attributed to dynamic recrystallization during ECAP processing. As previously discussed, continuous dynamic recrystallization in aluminum alloys typically occurs via an extended recovery process that involves the following steps: (1) multiplication of dislocations by Frank-Reed sources during plastic deformation, (2) formation of dislocation cells, (3) transformation of these cells into subgrains, (4) an increase in misorientations between subgrains due to addition plastic strain, and (5) gradual transformation of subgrains into main grains. Additionally, the intersection of micro-shear bands may play a significant role in grain refinement as documented in the literature [11-13]. Furthermore, Table 2 shows that increasing the processing temperature from 25  $^{\circ}\text{C}$  to 150  $^{\circ}\text{C}$  results in slight increase in grain size. This effect is likely due to the enhanced mobility of dislocations at higher temperatures, which reduces the number of locked dislocations and, consequently, limits the multiplication of dislocations via Frank-Reed sources. As a result, the rate of grain refinement with respect to plastic strain decreases as the deformation temperature increases [29, 30].



Fig. 2. Different SS specimens; from left to right: 1SS150, 2SS150, 4SS150, and 4SS25.

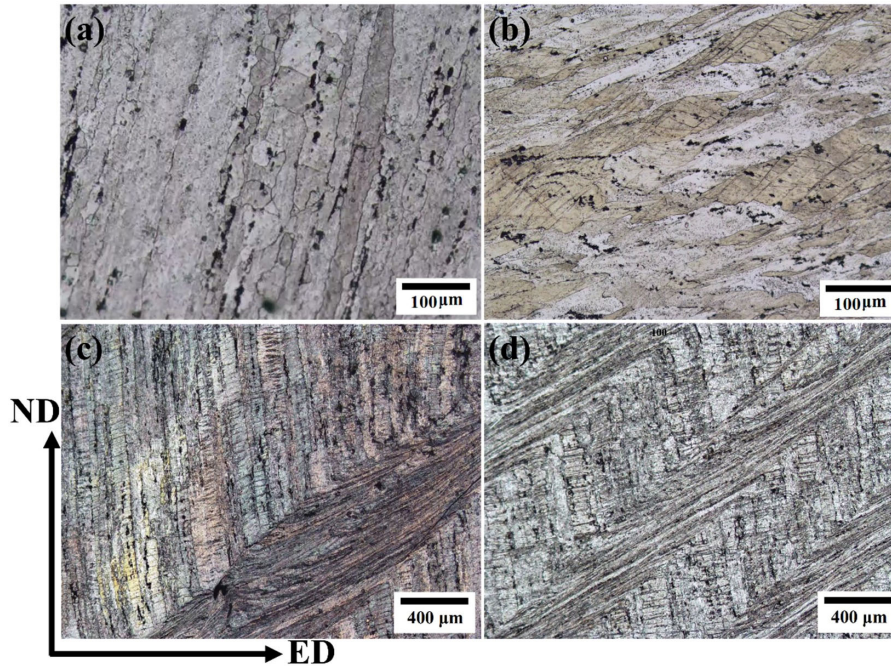


Fig. 3. Optical micrographs (OM) showing the microstructure of the alloy: (a) As solution treated, (b) 1SS25, (c) 2SS25, and (d) 2SS150.

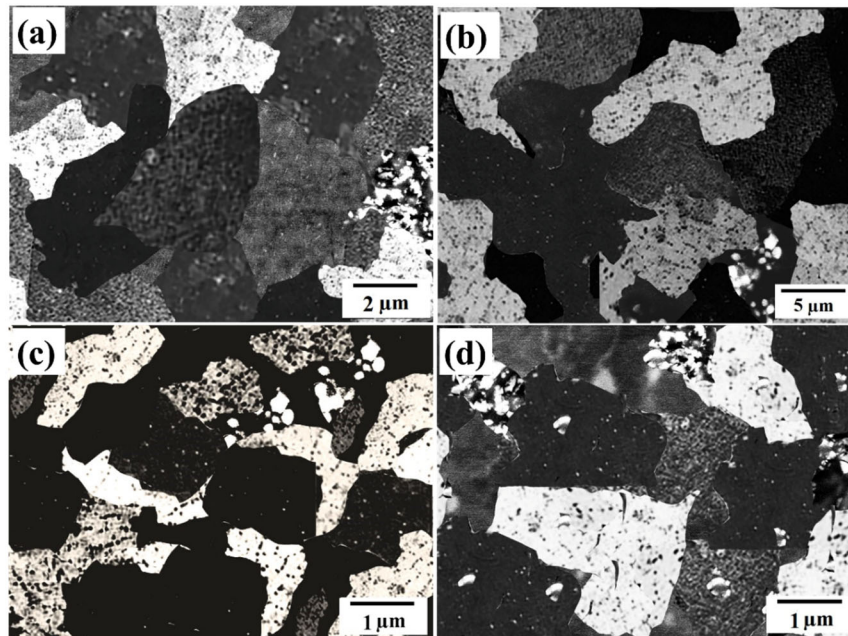


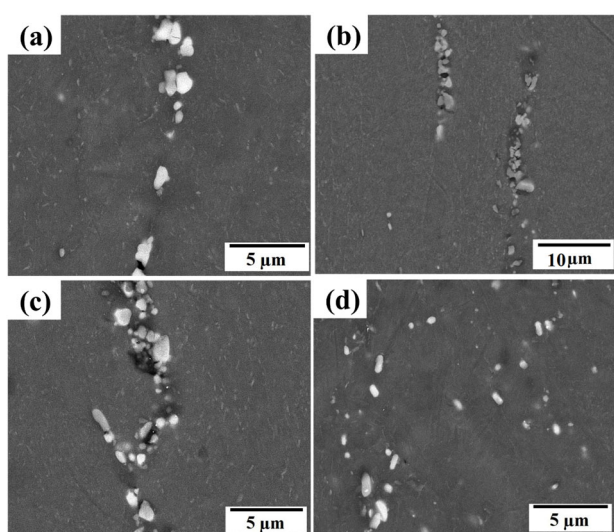
Fig. 4. FESEM-ECCI observed microstructure of: (a) 2OVG25, (b) 2OVG150, (c) 4OVG25, and (d) 4OVG150.

**Table 2.** Average grain size of the specimens observed by SEM-ECCI

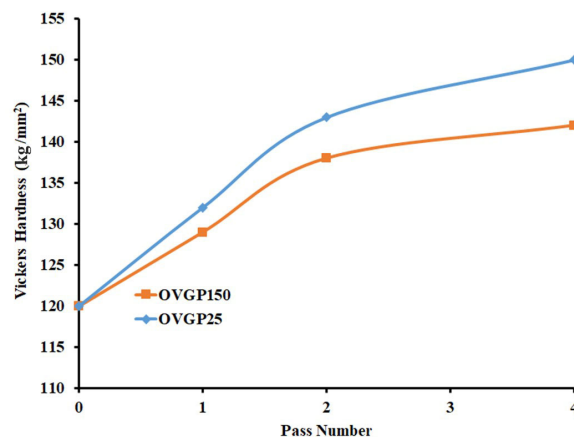
Specimen	2OVG25	4OVG25	2OVG150	4OVG150
Average grain size ( $\mu\text{m}$ )	3.03	0.92	3.68	1.15

Fig. 5 compares the precipitates in OVG-processed microstructures as observed by FESEM. As shown, the precipitates in these specimens are generally coarser than  $1\ \mu\text{m}$ , suggesting that they formed the pre-ECAP overaging treatment. In addition, a population of fine precipitates is visible in the ECAP-OVG processed specimens. These finer particles are likely the result of the partial dissolution and subsequent reprecipitation of coarse precipitates during ECAP, similar to previous reports [26, 31]. Overall, the data in Fig. 5 indicate that variations in ECAP pass number and processing temperature have a negligible effect on the precipitate's morphology in OVG-processed specimens.

Fig. 6 illustrates the effect of ECAP on the hardness of OVG specimens. The results show that the hardness increases significantly with up to two passes of ECAP at both processing temperatures. However, further ECAP passes yield only limited additional hardness. This behavior is attributed to supersaturation of grain refinement with increasing pass numbers as discussed in relation to Fig. 4.



**Fig. 5.** Appearance of precipitates in OVG-processed specimens: (a) 2OVG25, (b) 2OVG150, (c) 4OVG25 and (d) 4OVG150.



**Fig. 6.** Variation in Vickers hardness during ECAP processing using OVG procedures.

Previous studies have reported that dislocation accumulation and grain refinement become saturated when the imposed plastic strain reaches approximately 4-6, thereby reducing the rate of strengthening with additional passes [12-14, 29, 32]. Moreover, Fig. 6 indicates that specimens processed at  $150\ ^\circ\text{C}$  exhibit slightly lower hardness compared to those processed at  $25\ ^\circ\text{C}$ . This difference is likely due to the lower degree of grain refinement at the higher processing temperature, which enhances the mobility of dislocations, promoting temperature-activated dislocation annihilation. Consequently, the accumulation of dislocations and the rate of grain refinement decrease, leading to a reduced strengthening effect [12-15, 30].

#### 4. Conclusion

The effects of pre-deformation heat treatment and deformation regime on the behavior of AA2024 alloy during ECAP were investigated. The results indicated that overaging the alloy prior to processing is a more effective treatment compared to a solid solution treatment, which leads to fractures during multiple ECAP passes. Based on this study, the following conclusions can be drawn:

1. Imposing two passes of ECAP on solution treated AA2024 results in the appearance of macroscopic cracks, even at an elevated processing temperature of  $150\ ^\circ\text{C}$ .
2. A significant grain refinement is achieved by subjecting the overaged alloy to four passes of ECAP,

reducing the average grain size to approximately 1  $\mu\text{m}$ .  
3. Increasing the ECAP temperature from 25 °C to 150 °C has a limited effect on the overall behavior of the alloy.

### Acknowledgments

The authors gratefully acknowledge the Research Board of Ferdowsi University of Mashhad (FUM) for providing financial support and access to research facilities through grant No. 3/55745.

### Conflict of interest

The authors declare that they have completely followed publishing ethics and they have no conflict of interest.

### Data availability statement

The authors declare that the research data and analysis presented in this paper are available upon request.

### Funding

The authors declare that they have not received any funds, financial support, or grants from third parties for the research, authorship, and/or publication of this article.

### 5. References

- [1] Goodarzy, M. H., Arabi, H., Boutorabi, M. A., Seyedein, H. S., & Najafabadi, S. H. (2014). The effects of room temperature ECAP and subsequent aging on mechanical properties of 2024 Al alloy. *Journal of Alloys and Compounds*, 584, 753-759. <https://doi.org/10.1016/j.jallcom.2013.09.202>
- [2] Ringer, S. P., Sakurai, T., & Polmear, I. J. (1997). Origins of hardening in aged Al-Cu-Mg-(Ag) alloys. *Acta Materialia*, 45(9), 3731-3744. [https://doi.org/10.1016/S1359-6454\(97\)00039-6](https://doi.org/10.1016/S1359-6454(97)00039-6)
- [3] Hu, Z. Y., Fan, C. H., Tong, S., Ling, O. U., Dai, N. S., & Wang, L. (2021). Effect of aging treatment on evolution of S' phase in rapid cold punched Al-Cu-Mg alloy. *Transactions of Nonferrous Metals Society of China*, 31(7), 1930-1938. [https://doi.org/10.1016/S1003-6326\(21\)65627-3](https://doi.org/10.1016/S1003-6326(21)65627-3)
- [4] Yaghoubi, S., & Fereshteh-Saniee, F. (2022). A comprehensive study on soundness, microstructure, and uniformity of 2024 aluminum cups hydro-mechanically drawn at elevated temperatures. *The International Journal of Advanced Manufacturing Technology*, 120(11), 7905-7917. <https://doi.org/10.1007/s00170-022-09185-1>
- [5] Anijdan, S. M., Sadeghi-Nezhad, D., Lee, H., Shin, W., Park, N., Nayyeri, M. J., Jafarian, H. R. & Eivani, A. R. (2021). TEM study of S' hardening precipitates in the cold rolled and aged AA2024 aluminum alloy: influence on the microstructural evolution, tensile properties & electrical conductivity. *Journal of Materials Research and Technology*, 13, 798-807. <https://doi.org/10.1016/j.jmrt.2021.05.003>
- [6] Volokitina, I. (2020). Structure and mechanical properties of aluminum alloy 2024 after cryogenic cooling during ECAP. *Journal of Chemical Technology and Metallurgy*, 55(2), 479-485.
- [7] Dwivedi, S. S., Sharma, S., Li, C., Zhang, Y., Kumar, A., Singh, R., Eldin, S. M., & Abbas, M. (2023). Effect of nano-TiO<sub>2</sub> particles addition on dissimilar AA2024 and AA2014 based composite developed by friction stir process technique. *Journal of Materials Research and Technology*, 26, 1872-1881. <https://doi.org/10.1016/j.jmrt.2023.07.234>
- [8] Yuan, M., Wu, J., Meng, O., Zhang, C., Mao, X., Huang, S., & Wang, S. (2022). The Role of Al<sub>4</sub>C<sub>3</sub> morphology in tensile properties of carbon fiber reinforced 2024 aluminum alloy during thermal exposure. *Materials*, 15(24), 8828. <https://doi.org/10.3390/ma15248828>
- [9] Valiev, R. Z., & Langdon, T. G. (2006). Principles of equal-channel angular pressing as a processing tool for grain refinement. *Progress in Materials Science*, 51(7), 881-981. <https://doi.org/10.1016/j.pmatsci.2006.02.003>
- [10] Edalati, K., Ahmed A. Q., Akrami S., Ameyama, K., Aptukov, V., Asfandiyarov, R. N., Ashida, M., Astanin, V., Bachmaier, A., Beloshenko, V. and Bobruk, E. V. (2024). Severe plastic deformation for producing superfunctional ultrafine-grained and heterostructured materials: An interdisciplinary review. *Journal of Alloys and Compounds*. 1002, 174667. <https://doi.org/10.1016/j.jallcom.2024.174667>
- [11] Sakai, T., Belyakov, A., Kaibyshev, R., Miura, H. & Jonas, J. J. (2014). Dynamic and post-dynamic recrystallization under hot, cold and severe plastic deformation conditions. *Progress in Materials Science*, 60, 130-207. <https://doi.org/10.1016/j.pmatsci.2013.09.002>
- [12] Estrin, Y., & Vinogradov, A. (2013). Extreme grain refinement by severe plastic deformation: A wealth of challenging science. *Acta Materialia*, 61(3), 782–817. <https://doi.org/10.1016/j.actamat.2012.10.038>
- [13] Sabirov, I., Murashkin, M. Y., & Valiev, R. Z. (2013). Nanostructured aluminium alloys produced by severe plastic deformation: New horizons in development. *Materials Science and Engineering A*, 560, 1-24. <https://doi.org/10.1016/j.msea.2012.09.020>

- [14] Koizumi, T., & Kuroda, M. (2018). Grain size effects in aluminum processed by severe plastic deformation. *Materials Science and Engineering A*, 710, 300-308. <https://doi.org/10.1016/j.msea.2017.10.077>
- [15] Ma, K., Wen, H., Hu, T., Topping, T. D., Isheim, D., Seidman, D. N., Lavernia, E. J., & Schoenug, J. M. (2014). Mechanical behavior and strengthening mechanisms in ultrafine grain precipitation-strengthened aluminum alloy. *Acta Materialia*, 62, 141-155. <https://doi.org/10.1016/j.actamat.2013.09.042>
- [16] Khelfa, T., Rekik, M. A., Muñoz-Bolaños, J. A., Cabrera-Marrero, J. M. & Khitouni, M. (2018). Microstructure and strengthening mechanisms in an Al-Mg-Si alloy processed by equal channel angular pressing (ECAP). *International Journal of Advanced Manufacturing Technology*, 95, 1165-1177. <https://doi.org/10.1007/s00170-017-1310-1>
- [17] Bahadori-Fallah, J., Farshidi, M. H., & Kiani-Rashid, A. R. (2019). Equal channel angular pressing of spheroidal graphite cast iron. *Materials Research Express*, 6, 066542. <https://doi.org/10.1088/2053-1591/ab0dcf>
- [18] Askari Khan-Abadi, M., Farshidi, M. H., & Moayed, M. H. (2021). Microstructure evolution of the stainless steel 316L subjected to different routes of equal channel angular pressing. *Iranian Journal of Materials Forming*, 8(2), 4-11. <https://doi.org/10.22099/ijmf.2021.38714.1169>
- [19] Lee, W. B., & Chan, K. C. A. (1991). Microplasticity analysis of shear band cracks in rolled 2024 aluminium alloy. *International Journal of Fracture*. 52, 207-221. <https://doi.org/10.1007/BF00034905>
- [20] Bron, F., Besson, J., & Pineau, A. (2004). Ductile rupture in thin sheets of two grades of 2024 aluminum alloy. *Materials Science and Engineering A*, 380, 356-364. <https://doi.org/10.1016/j.msea.2004.04.008>
- [21] Sankaran, K. K. & Grant N. J. (1980). The structure and properties of splat-quenched aluminum alloy 2024 containing lithium additions. *Materials Science and Engineering*, 44(2), 213-227. [https://doi.org/10.1016/0025-5416\(80\)90122-6](https://doi.org/10.1016/0025-5416(80)90122-6)
- [22] Figueiredo, R. B., Cetlin, P. R., & Langdon, T. G. (2009). The evolution of damage in perfect-plastic and strain hardening materials processed by equal-channel angular pressing. *Materials Science and Engineering A*, 518, 124-131. <https://doi.org/10.1016/j.msea.2009.04.007>
- [23] Cetlin, P. R., Teresa, M., Aguilar, P., Figueiredo, R. B., & Langdon, T. G. (2010). Avoiding cracks and inhomogeneities in billets processed by ECAP. *Journal of Materials Science*. 45, 4561-4570. <https://doi.org/10.1007/s10853-010-4384-9>
- [24] Volokitina, I., Bychkov, A., Volokitin, A., & Kolesnikov, A. (2023). Natural aging of aluminum alloy 2024 after severe plastic deformation. *Metallography, Microstructure, and Analysis*, 12(3), 564-566. <https://doi.org/10.1007/s13632-023-00966-y>
- [25] Orozco-Caballero, A., Álvarez-Leal, M., Carreño, F., & Ruano, O. A. (2022). Superplastic behavior of overaged 2024 aluminum alloy after friction stir processing. *Metals*, 12(11), 1880. <https://doi.org/10.3390/met12111880>
- [26] Asadi, S., & Kazeminezhad, M. (2017). Multi directional forging of 2024 Al alloy after different heat treatments: microstructural and mechanical behavior. *Transaction of Indian Institute of Metals*, 70, 1707-1719. <https://doi.org/10.1007/s12666-016-0967-8>
- [27] Huang, Y., Robson, J. D., & Prangnell, P. B. (2010). The formation of nanograin structures and accelerated room-temperature theta precipitation in a severely deformed Al-4 wt.% Cu alloy. *Acta Materialia*, 58(5), 1643-1657. <https://doi.org/10.1016/j.actamat.2009.11.008>
- [28] Lee, S., Furukawa, M., Horita, Z., & Langdon, T. G. (2003). Developing a superplastic forming capability in a commercial aluminum alloy without scandium or zirconium additions. *Materials Science and Engineering A*, 342(1-2), 294-301. [https://doi.org/10.1016/S0921-5093\(02\)00319-2](https://doi.org/10.1016/S0921-5093(02)00319-2)
- [29] Renk, O., & Pippan, R. (2019). Saturation of grain refinement during severe [lastic deformation of single phase materials: reconsiderations, current status and open questions. *Materials Transactions*, 60(7), 1270-1282. <https://doi.org/10.2320/matertrans.MF201918>
- [30] Gong, Y. L., Wen, C. E., Wu, X. X., Ren, S. Y., Cheng, L. P., & Zhu, X. K. (2013). The influence of strain rate, deformation temperature and stacking fault energy on the mechanical properties of Cu alloys. *Materials Science & Engineering A*, 583, 199-204. <https://doi.org/10.1016/j.msea.2013.07.001>
- [31] Fan, C. H., Ling, O. U., Yang, Z. Y., Yang, J. J., & Chen, X. H. (2019). Re-dissolution and re-precipitation behavior of nano-precipitated phase in Al- Cu- Mg alloy subjected to rapid cold stamping. *Transactions of Nonferrous Metals Society of China*, 29(12), 2455-2462. [https://doi.org/10.1016/S1003-6326\(19\)65153-8](https://doi.org/10.1016/S1003-6326(19)65153-8)
- [32] Figueiredo, R. B., Kawasaki, M., & Langdon, T. G. (2023). Seventy years of Hall-Petch, ninety years of superplasticity and a generalized approach to the effect of grain size on flow stress. *Progress in Materials Science*, 137, 101131. <https://doi.org/10.1016/j.pmatsci.2023.101131>